

Nodeless superconducting gap in electron-doped $\text{BaFe}_{1.9}\text{Ni}_{0.1}\text{As}_2$ probed by quasiparticle heat transport

L. Ding,¹ J. K. Dong,¹ S. Y. Zhou,¹ T. Y. Guan,¹ X. Qiu,¹

C. Zhang,¹ L. J. Li,² X. Lin,² G. H. Cao,² Z. A. Xu,² S. Y. Li^{1,*}

¹*Department of Physics, Surface Physics Laboratory (National Key Laboratory), and Laboratory of Advanced Materials, Fudan University, Shanghai 200433, P. R. China*

²*Department of Physics, Zhejiang University, Hangzhou 310027, P. R. China*

(Dated: November 8, 2018)

The in-plane thermal conductivity κ of electron-doped iron-arsenide superconductor $\text{BaFe}_{1.9}\text{Ni}_{0.1}\text{As}_2$ ($T_c = 20.3$ K) single crystal was measured down to 70 mK. In zero field, the absence of a residual linear term κ_0/T at $T \rightarrow 0$ is strong evidence for nodeless superconducting gap. In magnetic field, κ_0/T shows a slow field dependence up to $H = 14.5$ T ($\approx 30\% H_{c2}$). This is consistent with the superconducting gap structure demonstrated by angle-resolved photoemission spectroscopy experiments in $\text{BaFe}_{1.85}\text{Co}_{0.15}\text{As}_2$ ($T_c = 25.5$ K), where isotropic superconducting gaps with similar size on hole and electron pockets were observed.

PACS numbers: 74.25.Fy, 74.25.Op, 74.25.Jb

The recent discovery of iron-based superconductors with T_c as high as 55 K [1, 2, 3, 4, 5] has attracted great attention. As a second family of high temperature superconductors after cuprates, the pairing symmetry of its superconducting gap is one of the most important issue to address. Spin triplet pairing was first ruled out in $\text{BaFe}_{1.8}\text{Co}_{0.2}\text{As}_2$ ($T_c = 22$ K) single crystal by the NMR Knight shift measurements [6]. This leaves three possible singlet pairing candidates: conventional s , d , and s_{\pm} , a superconducting state with order parameters of opposite signs on the electron and hole pockets [7]. While Andreev spectroscopy [8], angle-resolved photoemission spectroscopy (ARPES) [9, 10, 11, 12, 13, 14], and latest specific heat [15] experiments on FeAs-superconductors support full superconducting gaps without nodes, NMR data [16, 17, 18] and extensive penetration depth studies [19, 20, 21, 22, 23] reveal a contradictory picture of either nodeless or nodal superconductivity. Even if the nodeless superconducting gap is eventually confirmed, clear-cut experiments to distinguish s_{\pm} from conventional s -wave have to be done. Therefore, the pairing symmetry in iron-arsenide superconductors is still far from consensus.

Low-temperature thermal conductivity measurement is a powerful bulk tool to probe the superconducting gap structure [24]. For unconventional superconductors with nodes in the superconducting gap, like d -wave cuprates and p -wave ruthenate, the nodal quasiparticles will contribute a finite κ_0/T in zero field [25, 26]. So far, only one heat transport study was reported for FeAs-based superconductors [27]. For the hole-doped $\text{Ba}_{1-x}\text{K}_x\text{Fe}_2\text{As}_2$ ($T_c \simeq 30$ K) single crystal, a negligible κ_0/T was found in zero field, indicating a full superconducting gap. However, κ_0/T increases rapidly with magnetic field even for $H \ll H_{c2}$, which was inferred that the gap must be very small on some portion of the Fermi surface, whether from strong anisotropy or band dependence, or both. To clarify this important issue, more heat transport experiments

on other FeAs-based superconductors are needed.

In this Letter, we probe the superconducting gap of electron-doped $\text{BaFe}_{1.9}\text{Ni}_{0.1}\text{As}_2$ by measuring the thermal conductivity κ of a single crystal with $T_c = 20.3$ K down to 70 mK. In zero field, the residual linear term κ_0/T is negligible, a clear indication that $\text{BaFe}_{1.9}\text{Ni}_{0.1}\text{As}_2$ has nodeless superconducting gap. In magnetic field, $\kappa_0/T(H)$ shows a slow field dependence, different from the case of hole-doped $\text{Ba}_{1-x}\text{K}_x\text{Fe}_2\text{As}_2$. This difference is discussed on the base of superconducting gap structure in these two systems measured by ARPES.

Single crystals with nominal formula $\text{BaFe}_{1.9}\text{Ni}_{0.1}\text{As}_2$ were prepared by self flux method [28]. Energy Dispersive of X-ray (EDX) microanalysis show that the actual Ni content is 0.096, close to the nominal composition. The ac magnetization was measured in a Quantum Design Physical Property Measurement System (PPMS). The sample was cleaved to a rectangular shape of dimensions 1.5×0.88 mm² in the plane, with 55 μm thickness along the c -axis. Contacts were made directly on the fresh sample surfaces with silver paint, which were used for both resistivity and thermal conductivity measurements. The contacts are metallic with typical resistance 50 m Ω at 1.5 K. In-plane thermal conductivity was measured in a dilution refrigerator down to 70 mK, using a standard four-wire steady-state method with two RuO₂ chip thermometers, calibrated *in situ* against a reference RuO₂ thermometer. Magnetic fields were applied along the c -axis and perpendicular to the heat current. To ensure a homogeneous field distribution in the sample, all fields were applied at temperature above T_c .

Fig. 1a shows the in-plane resistivity of our $\text{BaFe}_{1.9}\text{Ni}_{0.1}\text{As}_2$ single crystal in zero field. The middle point of the resistive transition is at $T_c = 20.3$ K, in good agreement with previous study [28]. The 10-90% width of the resistive transition is less than 0.3 K, indi-

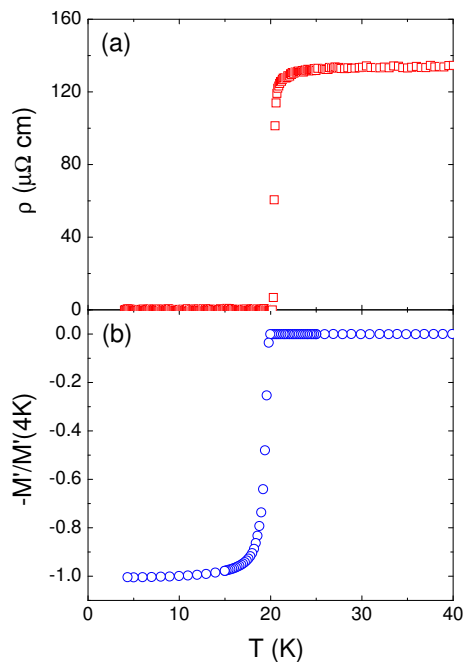


FIG. 1: (Color online) (a) In-plane resistivity $\rho(T)$ of $\text{BaFe}_{1.9}\text{Ni}_{0.1}\text{As}_2$ single crystal. The middle point of the resistive transition is at $T_c = 20.3$ K, and the 10-90% width of the transition is less than 0.3 K. (b) Normalized ac magnetization.

cating the high homogeneity of our crystal. The residual resistivity $\rho_0 = 132 \mu\Omega \text{ cm}$ is extrapolated from the data above T_c by using the Fermi liquid form $\rho = \rho_0 + AT^2$. In Fig. 1b, the normalized ac magnetization also shows a sharp superconducting transition similar to Fig. 1a.

In Fig. 2, the temperature dependence of the in-plane thermal conductivity for $\text{BaFe}_{1.9}\text{Ni}_{0.1}\text{As}_2$ in zero field is plotted as κ/T vs T . Since both electrons and phonons contribute to the measured conductivity, we fit the data to $\kappa/T = a + bT^{\alpha-1}$ [29, 30], where aT and bT^α represent electronic and phonon contributions, respectively. For phonon scattering off the crystal boundary at low temperature, one usually gets $\alpha = 3$, but specular reflection of phonons at the smooth crystal surfaces can result in a lower power $\alpha < 3$ [29, 30]. For $\text{BaFe}_{1.9}\text{Ni}_{0.1}\text{As}_2$, it is found that the data below 0.8 K can be well fitted (the solid line in Fig. 2) and gives $\kappa_0/T = -3 \pm 2 \mu\text{W K}^{-2} \text{ cm}^{-1}$, with $\alpha = 2.02 \pm 0.01$.

In the non-superconducting parent BaFe_2As_2 single crystal, the Wiedemann-Franz law, which relates charge and thermal conductivities by $\kappa/T = L_0/\rho$ with L_0 the Lorenz number $2.45 \times 10^{-8} \text{ W } \Omega \text{ K}^{-2}$, was found to be satisfied as $T \rightarrow 0$ [31]. For $\text{BaFe}_{1.9}\text{Ni}_{0.1}\text{As}_2$ with $T_c = 20.3$ K, the normal-state Wiedemann-Franz law expectation is $\kappa_0/T = L_0/\rho_0 = 0.186 \text{ mW K}^{-2} \text{ cm}^{-1}$ with $\rho_0 = 132 \mu\Omega \text{ cm}$, the dashed line in Fig. 2.

Since the residual linear term κ_0/T is within the experimental error bar $\pm 5 \mu\text{W K}^{-2} \text{ cm}^{-1}$ [30], which is less than 3% of the normal-state value, the electronic

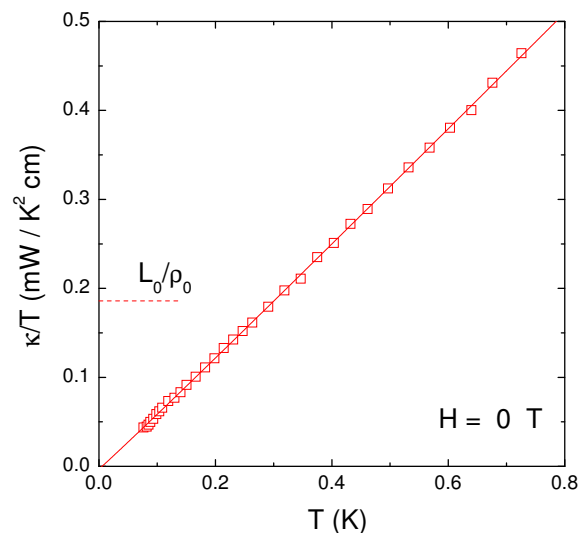


FIG. 2: (Color online) Temperature dependence of the in-plane thermal conductivity for $\text{BaFe}_{1.9}\text{Ni}_{0.1}\text{As}_2$ single crystal in zero field. The solid line represents a fit of the data to $\kappa/T = a + bT^{\alpha-1}$. This gives the residual linear term $\kappa_0/T = -3 \pm 2 \mu\text{W K}^{-2} \text{ cm}^{-1}$, which is negligible within the experimental error bar. The dashed line is the normal-state Wiedemann-Franz law expectation at $T \rightarrow 0$, namely L_0/ρ_0 , with L_0 the Lorenz number $2.45 \times 10^{-8} \text{ W } \Omega \text{ K}^{-2}$.

contribution to the thermal conductivity is negligible in zero field. This is consistent with previous results on hole-doped $\text{Ba}_{1-x}\text{K}_x\text{Fe}_2\text{As}_2$ single crystals [27] and the low- T_c superconductor BaNi_2As_2 ($T_c = 0.7$ K) [32], suggesting a nodeless (at least in ab -plane) superconducting gap. However, the power $\alpha = 2.02$ of the phonon conductivity bT^α is much lower than $\alpha = 2.65$ found in $\text{Ba}_{1-x}\text{K}_x\text{Fe}_2\text{As}_2$ [27]. We note that in the parent compound BaFe_2As_2 single crystal [31], the power $\alpha = 2.22$ is more closer to our value. Whether specular reflections of the phonon boundary scattering [29, 30] can give such a low α is not clear to us. In fact, phonons scattering off either electrons or grain boundaries will give $\alpha = 2$ [33]. Therefore, more experimental results are needed to clarify the temperature dependence of phonon thermal conductivity in FeAs-compound single crystals.

Fig. 3 shows the low-temperature thermal conductivity of $\text{BaFe}_{1.9}\text{Ni}_{0.1}\text{As}_2$ in magnetic fields applied along the c -axis ($H = 0, 9, 13,$ and 14.5 T). The data of κ/T in high fields below 0.25 K manifests similar temperature dependence to the zero field data. We fit the $H = 9, 13,$ and 14.5 T curves by using the same equation $\kappa/T = a + bT^{\alpha-1}$, with fixed $\alpha = 2.02$ due to the slightly increasing noise level of the in-field data. The solid lines are the fitting curves, which give $\kappa_0/T = 4, 15,$ and $20 \mu\text{W K}^{-2} \text{ cm}^{-1}$ for $H = 9, 13,$ and 14.5 T, respectively.

The upper critical field H_{c2} of $\text{BaFe}_{1.9}\text{Ni}_{0.1}\text{As}_2$ ($T_c = 20.3$ K) single crystal has not been determined yet. For $\text{BaFe}_{1.8}\text{Co}_{0.2}\text{As}_2$ ($T_c = 22$ K) single crystal, the H_{c2} was

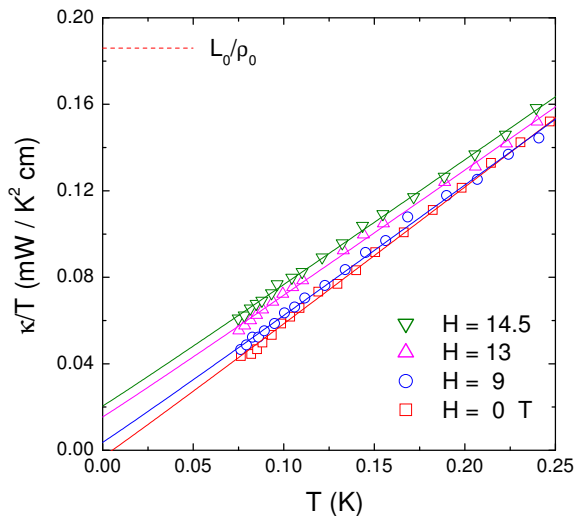


FIG. 3: (Color online) Low-temperature thermal conductivity of $\text{BaFe}_{1.9}\text{Ni}_{0.1}\text{As}_2$ in magnetic fields applied along the c -axis ($H = 0, 4, 9,$ and 14.5 T). The solid lines are $\kappa/T = a + bT^{\alpha-1}$ fits (see text). The dashed line is the normal state Wiedemann-Franz law expectation L_0/ρ_0 .

estimated ~ 50 T [34]. Taking this value as the H_{c2} of our $\text{BaFe}_{1.9}\text{Ni}_{0.1}\text{As}_2$ sample, $H = 14.5$ T is just about 30% of H_{c2} .

In Fig. 4, the normalized κ_0/T of $\text{BaFe}_{1.9}\text{Ni}_{0.1}\text{As}_2$ is plotted as a function of H/H_{c2} , together with the clean s -wave superconductor Nb [35], the dirty s -wave superconducting alloy InBi [36], the multi-band s -wave superconductor NbSe₂ [37], an overdoped sample of the d -wave superconductor Tl-2201 [25], and $\text{Ba}_{0.75}\text{K}_{0.25}\text{Fe}_2\text{As}_2$ [27]. For a clean (like Nb) or dirty (like InBi) type-II s -wave superconductor with isotropic gap, κ_0/T should grow exponentially with field (above H_{c1}). This usually gives negligible κ_0/T for field lower than $H_{c2}/4$, as seen in Fig. 4. For NbSe₂, κ_0/T increases much rapid at low field. This can be explained by its multi-gap structure, whereby the gap on the Γ band is approximately one third of the gap on the other two Fermi surfaces, and magnetic field will first suppresses the superconductivity on the Fermi surface with smaller gap (given that $H_{c2}(0) \propto \Delta_0^2$) [37].

As seen in Fig. 4, the $\kappa_0/T(H)$ of $\text{BaFe}_{1.9}\text{Ni}_{0.1}\text{As}_2$ more likely follows the behavior of isotropic s -wave gap. This field dependence is different from that of the hole-doped $\text{Ba}_{1-x}\text{K}_x\text{Fe}_2\text{As}_2$ ($T_c \simeq 30$ K) sample [27], where κ_0/T increases almost linearly with H up to 15 T. Such a rapid increase of $\kappa_0/T(H)$ in $\text{Ba}_{1-x}\text{K}_x\text{Fe}_2\text{As}_2$ has been interpreted as evidence for a k -dependent gap magnitude, coming from angle (*i.e.*, anisotropic) or band (*i.e.*, isotropic but with different magnetitudes on different bands) dependence, or both [27].

In order to explain this difference, let us examine the gap values on all Fermi surface (FS) sheets for both

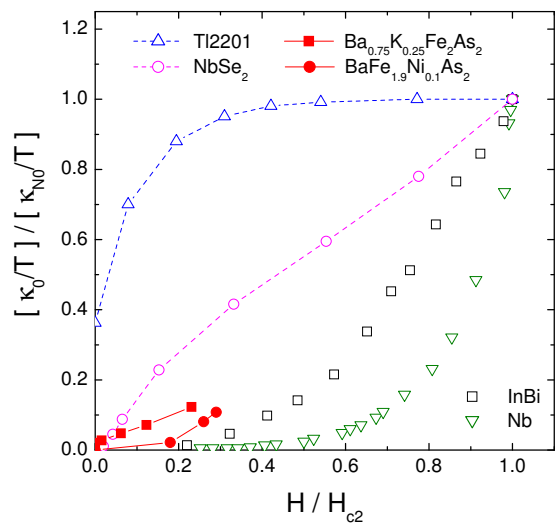


FIG. 4: (Color online) Normalized residual linear term κ_0/T of $\text{BaFe}_{1.9}\text{Ni}_{0.1}\text{As}_2$ as a function of H/H_{c2} . Similar data of the clean s -wave superconductor Nb [35], the dirty s -wave superconducting alloy InBi [36], the multi-band s -wave superconductor NbSe₂ [37], an overdoped sample of the d -wave superconductor Tl-2201 [25], and $\text{Ba}_{0.75}\text{K}_{0.25}\text{Fe}_2\text{As}_2$ [27] are also shown for comparison.

hole- and electron-doped BaFe_2As_2 measured by ARPES [9, 13, 14]. For hole-doped $\text{Ba}_{0.6}\text{K}_{0.4}\text{Fe}_2\text{As}_2$ ($T_c = 37$ K), the average gap values $\Delta(0)$ for the two hole (α and β) pockets are 12.5 and 5.5 meV, respectively, while for the electron (γ and δ) pockets, the gap value is about 12.5 meV [9, 13]. For electron-doped $\text{BaFe}_{1.85}\text{Co}_{0.15}\text{As}_2$ ($T_c = 25.5$ K), the average gap values $\Delta(0)$ of hole (β) and electron (γ and δ) pockets are 6.6 and 5.0 meV, respectively [14].

Since the doping level and T_c of our $\text{BaFe}_{1.9}\text{Ni}_{0.1}\text{As}_2$ sample are close to those of $\text{BaFe}_{1.85}\text{Co}_{0.15}\text{As}_2$, their superconducting gap structure should also be similar. Therefore, due to the similar sizes (6.6 vs 5.0 meV) of these isotropic superconducting gaps, the $\kappa_0/T(H)$ of our $\text{BaFe}_{1.9}\text{Ni}_{0.1}\text{As}_2$ sample behaves more like a conventional single-gap s -wave superconductor. For hole-doped $\text{Ba}_{0.6}\text{K}_{0.4}\text{Fe}_2\text{As}_2$, the sizes of these gaps are quiet different (12.5 vs 5.5 meV), which gives a ratio $R = 12.5/5.5 = 2.3$ [9, 13]. Taking this ratio for the slightly underdoped $\text{Ba}_{1-x}\text{K}_x\text{Fe}_2\text{As}_2$ [27], it is smaller than that in NbSe₂ ($R \approx 3$). This may explains the nearly linear increase of $\kappa_0/T(H)$ in $\text{Ba}_{1-x}\text{K}_x\text{Fe}_2\text{As}_2$ with the slope smaller than that in NbSe₂ [27], given $H_{c2}(0) \propto \Delta_0^2$ and magnetic field first suppresses the superconductivity on the Fermi surface with smallest superconducting gap.

In summary, we have used low-temperature thermal conductivity to clearly demonstrate nodeless superconducting gap in electron-doped iron-arsenide superconductor $\text{BaFe}_{1.9}\text{Ni}_{0.1}\text{As}_2$. Furthermore, the $\kappa_0/T(H)$ shows a slow H dependence at low field, different from the rapid, linear $\kappa_0/T(H)$ in hole-doped $\text{Ba}_{1-x}\text{K}_x\text{Fe}_2\text{As}_2$. This dif-

ference can be explained by the different ratio of the band-dependent superconducting gaps. Our results are consistent with nodeless multi-gaps in iron-arsenide superconductors, as revealed by ARPES experiments.

Note: After our present work first appeared on arXiv (0906.0138), two similar works on $\text{BaFe}_{2-x}\text{Co}_x\text{As}_2$ were also put on arXiv [38, 39]. In Ref. [38], a large κ_0/T was observed in $\text{BaFe}_{1.86}\text{Co}_{0.14}\text{As}_2$ single crystal at zero field, apparently contradicting to our results. In Ref. [39], the results of $\text{BaFe}_{2-x}\text{Co}_x\text{As}_2$ with $x = 0.148$ are consistent with ours.

This work is supported by the Natural Science Foundation of China, the Ministry of Science and Technology of China (National Basic Research Program No:2009CB929203 and 2006CB601003), Program for New Century Excellent Talents in University, and STCSM of China (No: 08dj1400200 and 08PJ1402100).

* E-mail: shiyan_li@fudan.edu.cn

-
- [1] Y. Kamihara *et al.*, J. Am. Chem. Soc. **130**, 3296 (2008).
 [2] X. H. Chen *et al.*, Nature **453**, 761 (2008).
 [3] G. F. Chen *et al.*, Phys. Rev. Lett. **100**, 247002 (2008).
 [4] Z. A. Ren *et al.*, Chin. Phys. Lett. **25**, 2215 (2008).
 [5] R. H. Liu *et al.*, Phys. Rev. Lett. **101**, 087001 (2008).
 [6] F. L. Ning *et al.*, J. Phys. Soc. Jap. **77**, 103705 (2008).
 [7] I. I. Mazin *et al.*, Phys. Rev. Lett. **101**, 057003 (2008).
 [8] T. Y. Chen *et al.*, Nature **453**, 1224 (2008).
 [9] H. Ding *et al.*, Europhys. Lett. **83** 47001 (2008).
 [10] T. Kondo *et al.*, Phys. Rev. Lett. **101**, 147003 (2008).
 [11] L. Zhao *et al.*, Chin. Phys. Lett. **25** 4402 (2008).
 [12] L. Wray *et al.*, Phys. Rev. B **78** 184508 (2008).
 [13] K. Nakayam *et al.*, arXiv:0812.0663.
 [14] K. Terashima *et al.*, arXiv:0812.3704.
 [15] G. Mu *et al.*, Phys. Rev. B **79**, 174501 (2009).
 [16] K. Matano *et al.*, Europhys. Lett. **83** 57001 (2008).
 [17] H. -J. Grafe *et al.*, Phys. Rev. Lett. **101**, 047003 (2008).
 [18] M. Yashima *et al.*, arXiv:0905.1896.
 [19] C. Martin *et al.*, arXiv:0807.0876.
 [20] K. Hashimoto *et al.*, Phys. Rev. Lett. **102**, 017002 (2009).
 [21] L. Malone *et al.*, arXiv:0806.3908.
 [22] C. Martin *et al.*, arXiv:0901.1804.
 [23] R. T. Gordon *et al.*, Phys. Rev. Lett. **102**, 127004 (2009).
 [24] H. Shakeripour *et al.*, New Journal of Physics **11**, 055065 (2009).
 [25] C. Proust *et al.*, Phys. Rev. Lett. **89**, 147003 (2002).
 [26] M. Suzuki *et al.*, Phys. Rev. Lett. **88**, 227004 (2002).
 [27] X. G. Luo *et al.*, arXiv:0904.4049.
 [28] L. J. Li *et al.*, New J. Phys. **11**, 025008 (2009).
 [29] M. Sutherland *et al.*, Phys. Rev. B **67**, 174520 (2003).
 [30] S. Y. Li *et al.*, Phys. Rev. B **77**, 134501 (2008).
 [31] N. Kurita *et al.*, arXiv:0904.4470.
 [32] N. Kurita *et al.*, Phys. Rev. Lett. **102**, 147004 (2009).
 [33] R. Berman, *Thermal conduction in Solids* (Oxford Univ. Press, Oxford) (1976).
 [34] A. Yamamoto *et al.*, Appl. Phys. Lett. **94**, 062511 (2009).
 [35] J. Lowell and J. Sousa, J. Low. Temp. Phys. **3**, 65 (1970).
 [36] J. Willis and D. Ginsberg, Phys. Rev. B **14**, 1916 (1976).
 [37] E. Boaknin *et al.*, Phys. Rev. Lett. **90**, 117003 (2003).
 [38] Y. Machida *et al.*, arXiv:0906.0508.
 [39] M. A. Tanatar *et al.*, arXiv:0907.1276.